Thermochimica Acta, 159 (1990) 109–123
Elsevier Science Publishers B.V., Amsterdam – Printed in The Netherlands

A STUDY OF THE THERMAL DECOMPOSITION OF CHROMIUM(II) OXALATE DIHYDRATE USING DIRECT CURRENT ELECTRICAL CONDUCTIVITY MEASUREMENTS

A.K. NIKUMBH *, M.M. RAHMAN and A.D. AWARE
Department of Chemistry, University of Poona, Pune 411 007 (India)
(Received 18 May 1989)

ABSTRACT

The feasibility of using direct current electrical conductivity measurements to study the solid state reactions involved in the preparation of chromium oxide from chromium(II) oxalate dihydrate has been analysed. Investigations were carried out using atmospheres of static air, dynamic air and dry nitrogen.

Study of the isothermal decomposition of chromium(II) oxalate dihydrate at different temperatures in these three atmospheres revealed that the anhydrous complex is formed first. This then undergoes oxidation decomposition to Cr_2O_3 with the probable formation of intermediates of CrO and Cr_3O_4 (i.e. $CrO_{1.33}$) along with the anhydrous complex. The conductivity measurements were supplemented with data obtained by chemical, thermal (TG, DTG and DTA), IR spectroscopic and X-ray powder diffraction analyses. The gaseous decomposition products were characterized by gas–liquid chromatography.

INTRODUCTION

The thermal decomposition of metal hydroxides, metal hydrous oxides and metal carboxylates has become an important area of research in the fields of catalysis, surface chemistry [1,2] and magnetic oxides [3–6]. The process can involve many complicated steps, such as oxidation or reduction, atomic diffusion, recrystallization, sintering, etc. Moreover, oxidation or reduction of metal ions may also occur, depending on the atmosphere. Among the studies of this kind that have been carried out on chromium compounds, hydrous Cr_2O_3 has been most widely investigated [7,8] because its principal decomposition product, Cr_2O_3, has applications as an oxidation or reduction catalyst. The thermal decomposition of bivalent and trivalent metal carboxylates has also been investigated extensively [9–15].

* Address for correspondence: Dr. A.K. Nikumbh, Department of Chemistry, University of Poona, Ganeshkhind, Pune 411 007, India.

0040-6031/90/$03.50

Interest has recently been shown in the use of electrical conductivity techniques in the study of solid state decomposition reactions [3–6]. The present work is concerned with the feasibility of using direct current electrical conductivity measurements as a probe to study the progress of the thermal decomposition of chromium(II) oxalate dihydrate. The conductivity measurements were supplemented with data obtained by TG, DTG and DTA, X-ray diffraction, IR spectroscopy and gas–liquid chromatography.

EXPERIMENTAL

Sample preparation

Chromium(II) oxalate dihydrate was prepared according to the usual procedure, as described in refs. 16 and 17. A dry mixture of 14 g of $CrSO_4 \cdot 5H_2O$ [16], 8 g of $Na_2C_2O_4$ and 0.25 g of $H_2C_2O_4 \cdot 2H_2O$ was placed in a three-necked flask under a stream of dry nitrogen. 150 ml of oxygen-free water was then added, and the mixture stirred vigorously with a magnetic stirrer. After some time, chromium(II) oxalate dihydrate, $CrC_2O_4 \cdot 2H_2O$, separated out as a fine crystalline yellowish-green precipitate. This was filtered, washed with cold water and dried in vacuo.

Elemental analyses indicated the composition of the oxalate to be: Cr, 28.98 wt.%; C, 13.54 wt.%; H, 2.25 wt.%. The calculated values are: Cr, 29.39 wt.%; C, 13.63 wt.%; H, 2.27 wt.%. The IR spectrum showed frequencies corresponding to oxalate group, hydroxyl group, metal oxygen, etc. The bidentate linkage of the oxalate group with the metal was confirmed on the basis of the difference between the anti-symmetric and symmetric stretching frequencies. The X-ray diffraction pattern showed the sample to be polycrystalline in nature, with low symmetry. The two molecules of water of crystallization were confirmed on the basis of thermal analysis curves and d.c. electrical conductivity measurements. $CrC_2O_4 \cdot 2H_2O$ has a magnetic moment of 4.65 B.M., which indicates that the compound has free spin with sp^3d^2 hybridization. For the study of the decomposition of the oxalate in dynamic air, an air compressor was used to maintain an air-flow of between 80 and 85 ml min^{-1}.

X-ray diffraction analysis

The products of decomposition of $CrC_2O_4 \cdot 2H_2O$ were analysed by X-ray powder diffraction techniques, using Cu $K\alpha$ radiation (wavelength = 0.709 Å, nickel filter) and a PW 1730 Philips X-ray diffractometer. The experimentally observed *d*-spacing values and relative intensities were compared with those reported in the ASTM File.

IR spectroscopic analysis

IR spectra were recorded using a Perkin–Elmer Model 337 spectrophotometer with a Nujol mull.

Thermal analysis

Thermal analysis curves were recorded using a Netzsch instrument, for atmospheres of static air, dynamic dry nitrogen and dynamic air. The flow rate for the dynamic dry nitrogen and dynamic air was 90 ml min^{-1}. The heating rate was 3 °C min^{-1} for the static air and 5 °C min^{-1} for the runs with dynamic air and dynamic dry nitrogen.

Direct current electrical conductivity measurements

The d.c. electrical conductivity was measured using a Philips PP 9004 microvoltmeter [3]. The conductivity cell was designed so that different atmospheres could be used. For the decomposition study, the heating rate was adjusted to 3 °C min^{-1}. Precautions were taken to maintain a constant rate of heating. The results, presented in terms of log σ vs. $10^3\ T^{-1}$ (in K^{-1}), are given in Figs. 1–4 below. The data were obtained using four different pellets of the same sample, and the patterns of the σ vs. T^{-1} plots were found to be reproducible to within ± 1 °C.

The evolution of various gases during the thermal decomposition of $CrC_2O_4 \cdot 2H_2O$ was recorded using Shimadzu RIA and Hewlett-Packard instruments, with nitrogen as the carrier gas.

RESULTS AND DISCUSSION

Static air atmosphere

The TG, DTG and DTA curves for $CrC_2O_4 \cdot 2H_2O$ are shown in Fig. 1a. Dehydration of $CrC_2O_4 \cdot 2H_2O$ was indicated by an endothermic peak in the DTA and DTG curves at 140 °C. The TG curve showed a weight loss within the range 70–200 °C, with a plateau up to 290 °C corresponding to the loss of two water molecules (calc., 20.4%; found, 20.1%). There was a sharp exothermic peak (at 320 °C) between 290 and 380 °C in the DTA curve and a sharp endothermic peak (at 328 °C) between 300 and 400 °C in the DTG curve, corresponding to the oxidative decomposition of CrC_2O_4 to Cr_2O_3. The TG curve showed a continuous weight loss within the temperature range 290–550 °C, corresponding to the formation of Cr_2O_3 (calc., 45.17%; found, 45.46%) as final product.

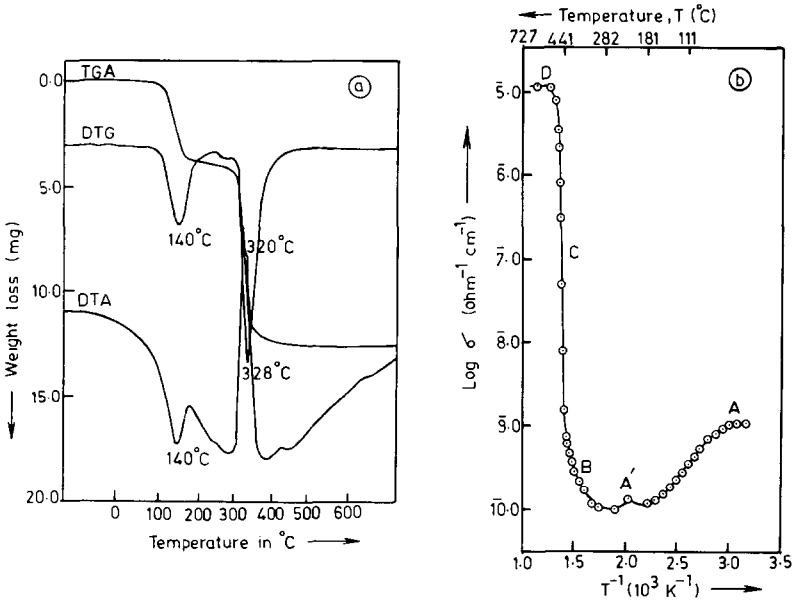

Fig. 1. Static air atmosphere: a, TG, DTA and DTG curves for $CrC_2O_4 \cdot 2H_2O$; b, plot of log σ vs. T^{-1} for $CrC_2O_4 \cdot 2H_2O$.

A comparison of the findings of conventional thermal analysis with those of conductivity analysis reveals that conductivity analysis gives a much more detailed view of the decomposition process. The temperature variation of electrical conductivity σ (Fig. 1b) did not show much change with the increse in temperature from 27 to 100 °C (Region A). There was a steady decrease in σ between 90 and 210 °C and the value then remained nearly constant up to 260 °C (Region A′). There was a steady increase in σ between 270 and 390 °C (Region B), followed by a steep increase at 400 °C, to a maximum at 465 °C (Region C). The σ value then increased steadily and remained almost constant within the temperature range 500–600 °C (Region D).

The plot of log σ vs. T^{-1} indicated that the decomposition of $CrC_2O_4 \cdot 2H_2O$ proceeds via the formation of intermediates of varying conductivity, whereas the TG curve obtained by conventional thermal analysis showed only a continuous weight loss, and the DTA curve showed only one sharp exothermic peak, corresponding to oxidative decomposition.

Analysis of the plot of log σ vs. T^{-1} must include due consideration of the physical factors involved in the transformation of a compound (formed during a chemical reaction) in the amorphous phase of fusion layers to large crystallites, through the probable intermediate stages, such as the formation of a fine network of grain boundaries and subsequent consolidation, and the formation of defects and subsequent annealing of such defects. It is therefore necessary to supplement the electrical conductivity measurements with

TABLE 1

X-ray diffraction data for $CrC_2O_4 \cdot 2H_2O$ [a]

Observed *d*-spacing values (present study) (Å)	Observed *d*-spacing values (present study) (Å)
4.68 (100)	2.14 (10)
3.87 (25)	2.09 (5)
3.54 (10)	2.03 (5)
2.95 (38)	1.95 (5)
2.64 (9)	1.90 (10)
2.58 (14)	1.89 (12)
2.37 (6)	1.79 (10)
2.24 (8)	1.59 (4)
2.15 (3)	

[a] The figures given in brackets are intensities relative to the linewidth intensity (100).

other measurements of the structural characteristics of the samples, such as measurements of IR spectra and X-ray diffraction patterns.

Within Region A of Fig. 1b there was no observable change in the X-ray diffraction pattern (Table 1) or the IR spectra for the sample heated isothermally. The IR bands characteristic of the co-ordinated oxalate group [18,19], at 1600(s) (this band was broad, owing to overlap with the H_2O band), 1350(m), 1210(m), 815(s) and 488(m) cm^{-1}, persisted for samples heated up to 120 °C. In addition, bands due to co-ordinated water molecules were observed at 3340(s), 1640(s), 725(m), 580(m) and 535(m) cm^{-1}. The findings of elemental analysis were in good agreement with the formula $CrC_2O_4 \cdot 2H_2O$.

Within the temperature range corresponding to Region A′ in Fig. 1b, the IR spectra of samples heated at 190 °C gave decisive results. An additional band appeared at 793 cm^{-1}, the intensity of which increased with increasing temperature; and a corresponding decrease was observed in the intensity of the band at 814 cm^{-1} (see Fig. 2). At 250 °C the band at 814 cm^{-1} had disappeared completely and the band at 795 cm^{-1} had become strong and narrow. Other oxalate group bands observed for the parent compound also showed a shift: the band at 488 cm^{-1} shifted by +8 cm^{-1}, the band at 1310 cm^{-1} by +5 cm^{-1}, the band at 1350 cm^{-1} by +9 cm^{-1}, and the band at 1600 cm^{-1} by about +35 cm^{-1}. A comparison of the group frequencies of water molecules indicated that the sample heated at 250 °C did not contain any water molecules. Region A′ of the plot of log σ vs. T^{-1} shown in Fig. 1b can therefore be related to dehydration of the oxalate. Such a change is probably associated with a change from the octahedral geometry of chromium(II) to a tetrahedral form. The colour of the compound changed from yellowish-green at room temperature to gray at 250 °C. Supplementary elemental and oxalate group analyses indicated that the sample obtained at

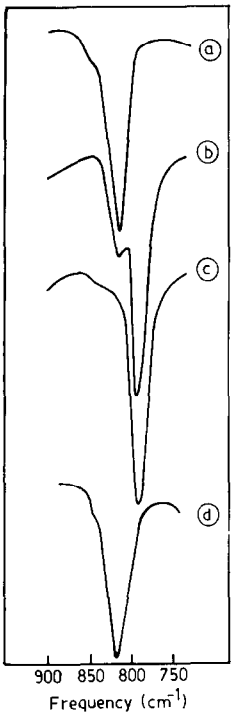

Fig. 2. IR spectra for chromium(II) oxalate within the region 900–750 cm^{-1} after samples had equilibrated at various temperatures, and then been brought to room temperature in an atmosphere of nitrogen: a, t = room temperature; b, $t = 190\,^{\circ}C$; c, $t = 250\,^{\circ}C$; d, sample treated as c, but exposed to water vapour at room temperature for 30 h.

250 °C was predominantly composed of anhydrous oxalate complex. To confirm these results, the sample heated at 250 °C was exposed to water vapour in a desiccator at room temperature. IR spectra taken at various time intervals showed that about 30 h are required for the conversion of CrC_2O_4 to $CrC_2O_4 \cdot 2H_2O$ (Curve d, Fig. 2). The X-ray diffraction pattern also showed broad peaks with no observable change (Table 2).

After the dehydration step, the value of σ increased steadily from 270 to 390 °C (Region B). The IR spectra of the sample of $CrC_2O_4 \cdot 2H_2O$ heated isothermally at 350 °C showed a decrease in the intensity of the co-ordinated oxalate band. Bands also appeared at 630 and 498 cm^{-1} for metal–oxygen stretching frequencies which were due to the presence of chromium oxide [20]. The X-ray diffraction pattern of this isothermally heated sample (Table 3) showed a generally sharp line, indicating that the sample was predominantly crystalline. The pattern corresponded to anhydrous CrC_2O_4 and CrO [21].

A sharp increase in the value of σ was observed within the temperature range 400–465 °C (Region C, Fig. 1b). For the sample heated isothermally at 440 °C, the IR spectra did not show any band corresponding to the

TABLE 2

X-ray diffraction data for anhydrous CrC_2O_4 obtained from $CrC_2O_4 \cdot 2H_2O$ by heating in an atmosphere of nitrogen at 250 °C [a]

Observed *d*-spacing values (present study) (Å)	Observed *d*-spacing values (present study) (Å)
4.69 (100)	2.48 (40)
3.76 (60)	2.16 (20)
2.90 (30)	1.89 (12)
2.75 (25)	1.74 (15)
2.60 (51)	1.63 (20)
	1.56 (25)
	1.38 (7)

[a] The figures given in brackets are intensities relative to the linewidth intensity (100).

oxalate group, but a strong and broad band was observed at 500 cm^{-1}. The X-ray diffraction pattern of this isothermally heated sample was complex, probably corresponding to a mixture of CrO, Cr_3O_4 and Cr_2O_3. Thus the steep increase in conductivity observed in Region C was due to the transformation of CrC_2O_4 to Cr_3O_4 (i.e. $CrC_{1.33}$), possibly via the semi-conducting

TABLE 3

X-ray diffraction data for CrC_2O_4 and CrO obtained from $CrC_2O_4 \cdot 2H_2O$ by heating in an atmosphere of static air at 350 °C [a]

Observed *d*-spacing values (present study) (Å)	CrO *d*-spacing values [b] (Å)
4.66 (60)	
3.72 (20)	
2.93 (30)	2.95 (40)
2.90 (21)	
2.78 (21)	
2.50 (100)	2.52 (100)
2.31 (12)	
2.10 (25)	2.09 (40)
1.89 (10)	
1.70 (20)	1.71 (20)
1.62 (10)	1.61 (40)
1.47 (61)	1.49 (60)
1.37 (10)	
1.30 (5)	1.28 (20)
1.08 (8)	1.088 (20)
0.91 (11)	
0.82 (15)	0.81 (20)

[a] The figures given in brackets are intensities relative to the linewidth intensity (100).
[b] Ref. 21.

TABLE 4

X-ray diffraction data for Cr_2O_3 obtained from $CrC_2O_4 \cdot 2H_2O$ by heating in an atmosphere of nitrogen at 530 °C [a]

Observed *d*-spacing values (present study) (Å)	Cr_2O_3 *d*-spacing values [b] (Å)
4.64 (14)	
3.64 (40)	3.63 (75)
2.94 (40)	
2.78 (32)	
2.65 (80)	2.66 (100)
2.49 (100)	2.48 (95)
	2.176 (40)
2.07 (16)	2.048 (10)
1.90 (7)	1.81 (40)
1.65 (55)	1.67 (90)
	1.58 (14)
1.47 (49)	1.46 (25)
1.42 (11)	1.43 (40)
1.27 (7)	1.29 (20)
	1.24 (18)
	1.21 (8)
	1.17 (14)
	1.15 (10)
	1.12 (10)
1.09 (15)	1.08 (18)
1.04 (6)	1.04 (16)
1.00 (5)	0.94 (14)
	0.86 (25)

[a] The figures given in brackets are intensities relative to the linewidth intensity (100).
[b] Ref. 23.

CrO. It has been reported in the literature [22] that the electrical conductivity increases with decreasing O/Cr ratio. In the present work, no separate step was identified for the formation of CrO. It should be noted here that the conductivity data were obtained from a dynamic system, while the other data were obtained for samples which had been subjected to isothermal heating at a specified temperature.

Within the temperature range of Region D in Fig. 1b, the value of σ remained almost constant. The X-ray diffraction pattern observed for this region indicated a predominance of Cr_2O_3 (Table 4). Thus the conductivity measurements, supplemented with IR spectral data, X-ray diffraction patterns and elemental analysis, allowed a detailed analysis of the thermal decomposition of $CrC_2O_4 \cdot 2H_2O$.

When the reaction is carried out in an atmosphere of normal air, the gaseous product acts as a gas buffer for the solid state reaction and some of the reactions are poorly defined. Clarification of e.g. the role of co-ordinated

water molecules in $CrC_2O_4 \cdot 2H_2O$ or of atmospheric oxygen in the solid state reaction carried out in static air can be achieved by comparing data relating to various physical properties with data obtained for the same reaction carried out in a dynamic atmosphere of dry nitrogen.

Dynamic nitrogen atmosphere

The dehydration of $CrC_2O_4 \cdot 2H_2O$ (Fig. 3a) was clearly indicated by an endothermic peak in the DTA curve at 140 °C and a peak at the same temperature in the DTG curve. The TG curve showed weight loss within the temperature range 65–208 °C with a plateau up to 310 °C corresponding to the loss of two water molecules (calc., 20.35%; found, 20.45%). The decomposition of the oxalate (CrC_2O_4) was indicated by an endothermic peak in the DTA curve at 400 °C and in the DTG curve at the same temperature. The TG curve showed a continuous weight loss from 310 to 590 °C. This weight loss was found to be in good agreement with the formation of Cr_2O_3 (calc., 45.37%; found, 45.58%) as final product.

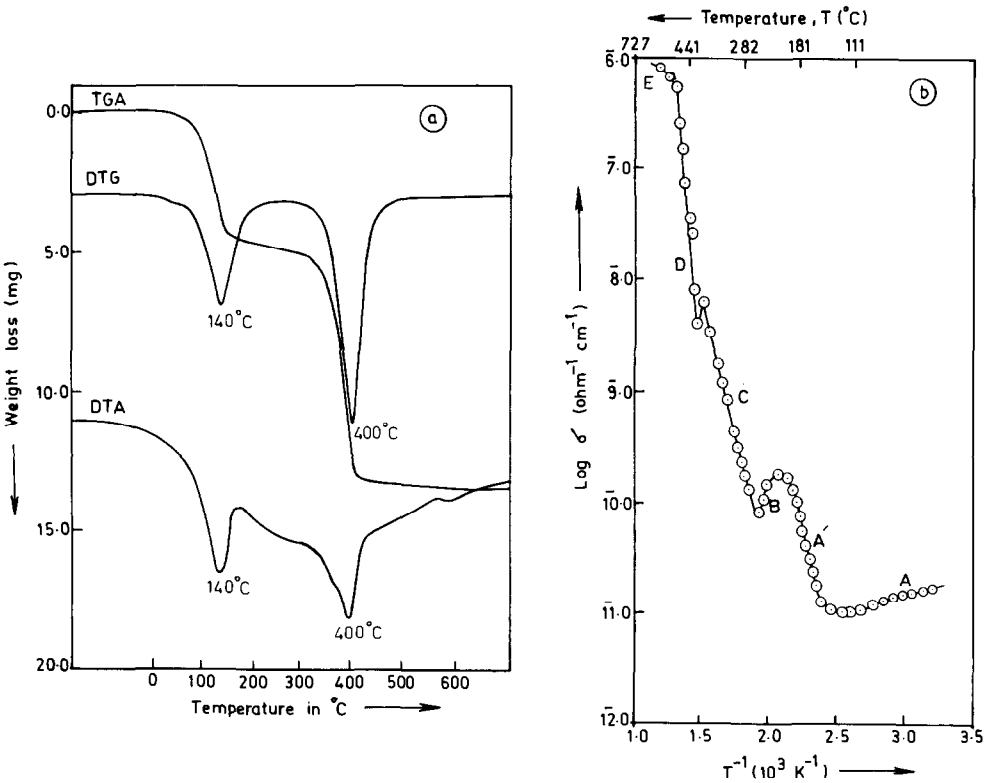

Fig. 3. Dynamic nitrogen atmosphere: a, TG, DTA and DTG curves for $CrC_2O_4 \cdot 2H_2O$; b, plot of log σ vs. T^{-1} for $CrC_2O_4 \cdot 2H_2O$.

The plot of log σ vs. T^{-1} (Fig. 3b) showed that σ was initially constant (Region A), but then increased steadily to a maximum at 210 °C (Region A′). IR spectral and X-ray diffraction data indicated no observable change in the isothermally heated sample of $CrC_2O_4 \cdot 2H_2O$ for this region. The value of σ then decreased linearly between 210 and 270 °C (Region B). The IR spectrum of the sample taken at 255 °C showed no H–OH bands. Elemental analysis agreed well with the anhydrous compound CrC_2O_4, and the X-ray diffraction pattern indicated that the sample was less crystalline than the parent compound $CrC_2O_4 \cdot 2H_2O$ (Table 2). Region B can therefore be said to correspond to the dehydration of $CrC_2O_4 \cdot 2H_2O$.

After the dehydration step, the value of σ increased steadily within the temperature range 270–410 °C (Region C), showing a kink at 390 °C. IR spectra for a sample heated isothermally in this region showed bands attributable to Cr–O stretching frequencies becoming more intense and bands relating to co-ordinated carboxylate decreasing in intensity. The X-ray diffraction pattern showed sharp lines, indicating that the sample was predominantly crystalline. The pattern fitted with data for anhydrous CrC_2O_4 and CrO [21].

A steep increase in σ was observed within the temperature range 410–470 °C, in Region D (Fig. 3b). A sample obtained by isothermal heating in dry nitrogen at 450 °C was probably a mixture of Cr_3O_4 and Cr_2O_3. The X-ray diffraction pattern (Table 5) was generally broad, and comparable with data reported for Cr_3O_4 [24] and Cr_2O_3 [23].

X-ray diffraction pattern data for a sample from the dry nitrogen atmosphere run obtained at 510 °C (Region E) showed sharp lines and were comparable with the data reported [23] for Cr_2O_3 (Table 4). No line which could be assigned to metallic chromium could be detected in our findings. Thus X-ray diffraction patterns and conductivity measurements (10^{-6} Ω^{-1} cm) [22] suggested that the product obtained by thermal decomposition of $CrC_2O_4 \cdot 2H_2O$ in a dry nitrogen atmosphere is pure Cr_2O_3.

Although the nature of the decomposition process and the final products from $CrC_2O_4 \cdot 2H_2O$ in static air and dynamic (dry and pure) nitrogen atmospheres were similar, a few critical differences were observed.

(a) The temperatures corresponding to dehydration and decomposition from DTA and DTG curves under nitrogen atmosphere were resolvable and matched changes observed in plots of log σ vs. T^{-1}; whereas the curves obtained under static air were quite complex.

(b) The decomposition temperatures observed from DTA and DTG curves under nitrogen atmosphere were higher than those observed under static air.

(c) Oxalate was intimately associated with the decomposed product up to 390 °C in dry nitrogen and static air.

(d) The step corresponding to the formation of anhydrous CrC_2O_4 was resolved in the plot of log σ vs. T^{-1} for the dry nitrogen atmosphere.

TABLE 5

X-ray diffraction data for Cr_3O_4 obtained from $CrC_2O_4 \cdot 2H_2O$ by heating in an atmosphere of nitrogen at 450 °C [a]

Observed *d*-spacing values (present study) (Å)	Cr_3O_4 *d*-spacing values [b] (Å)
4.72 (25)	4.78 (40)
3.66 (20)	
3.20 (13)	
2.91 (20)	2.86 (40)
2.80 (28)	
2.66 (46)	
2.59 (100)	2.58 (100)
2.48 (60)	
2.35 (35)	2.39 (20)
2.26 (10)	
2.15 (11)	2.16 (60)
1.88 (15)	1.90 (20)
1.77 (21)	1.73 (30)
1.61 (50)	1.65 (90)
	1.59 (20)
1.51 (12)	1.53 (60)
1.45 (50)	1.43 (80)
1.38 (5)	1.35 (10)
	1.287 (30)
1.26 (16)	1.280 (50)
	1.22 (10)
1.17 (14)	
1.087 (18)	
0.890 (22)	

[a] The figures given in brackets are intensities relative to the linewidth intensity (100).
[b] Ref. 24.

Since the solid state thermal decomposition of $CrC_2O_4 \cdot 2H_2O$ is influenced by the atmosphere, it was decided to undertake similar measurements in other controlled atmospheres.

Dynamic air atmosphere

The TG curve showed a weight loss between 75 and 240 °C (Fig. 4a). The DTA curve showed an endothermic peak at 140 °C and there was also a peak in the DTG curve at the same temperature, corresponding to the dehydration of $CrC_2O_4 \cdot 2H_2O$, and an exothermic peak at 304 °C, corresponding to oxidative decomposition.

Region A′ in the plots of log σ vs. T^{-1} (Fig. 4b) corresponds to the dehydration of $CrC_2O_4 \cdot 2H_2O$. There was a steep increase in σ at 280 °C followed by another steep increase at 370 °C (see Regions B and C, Fig. 4b).

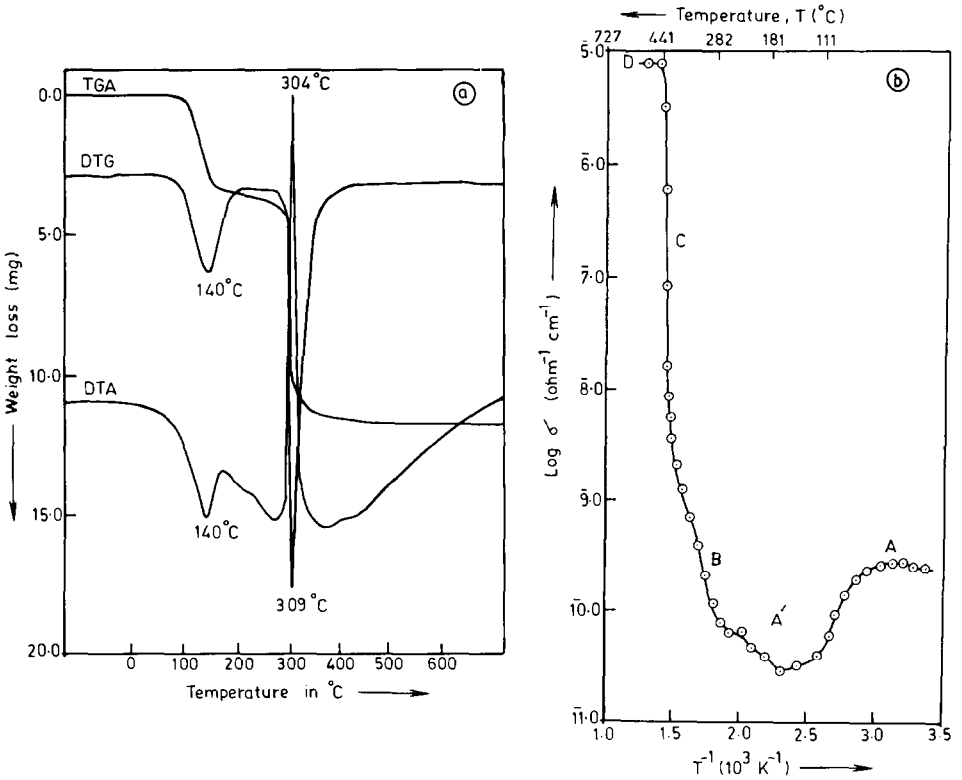

Fig. 4. Dynamic air atmosphere: a, TG, DTA and DTG curves for $CrC_2O_4 \cdot 2H_2O$; b, plot of log σ vs. T^{-1} for $CrC_2O_4 \cdot 2H_2O$.

These two temperature ranges, 280–370 and 370–440 °C, can be tentatively assigned to the formation of CrO and Cr_3O_4, respectively. However, our repeated experiments to obtain pure CrO by careful heating in dynamic air, even at 290 °C, always led to the formation of a mixture of CrO and CrC_2O_4 (see Table 3). Since the X-ray diffraction pattern of the sample obtained in this way displayed broad lines, the product seems to be less crystalline. The IR spectrum of a sample heated isothermally in Regions B and C showed broad peaks at 905, 625 and 490 cm^{-1} which were due to Cr–O stretching frequencies [20]. Within the temperature range ($\sim$ 510 °C) of Region D in Fig. 4b, the value of σ remained almost constant. The X-ray diffraction pattern for this region indicated a predominance of Cr_2O_3.

The gaseous products obtained by the thermal decomposition of $CrC_2O_4 \cdot 2H_2O$ under dynamic (pure and dry) nitrogen atmosphere were indicated by the chromatograms shown in Fig. 5. These chromatograms showed the presence of polar type gases (namely, CO, CO_2, H, etc.). The gases were collected at around 350 °C.

Let us now analyse the different paths by which the decomposition of $CrC_2O_4 \cdot 2H_2O$ takes place in different atmospheres. Complete dehydration

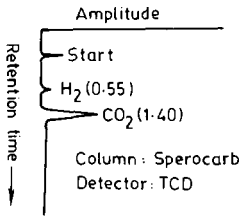

Fig. 5. Gas–liquid chromatograms for the gases obtained during the thermal decomposition of $CrC_2O_4 \cdot 2H_2O$ in a dynamic nitrogen atmosphere.

$$CrC_2O_4 \cdot 2H_2O \xrightarrow{100\text{–}270\,^\circ C} CrC_2O_4 + 2H_2O\uparrow$$

$$CrC_2O_4 \xrightarrow{270\text{–}400\,^\circ C} CrO + CO\uparrow + CO_2\uparrow$$

$$CrO + 2CrC_2O_4 \xrightarrow{400\text{–}465\,^\circ C} Cr_3O_4 + 4CO\uparrow + [O]$$

$$2Cr_3O_4 + [O] \xrightarrow{510\,^\circ C} 3Cr_2O_3$$

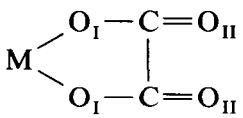

Scheme 1.

of $CrC_2O_4 \cdot 2H_2O$ was observed under static air, dynamic dry nitrogen and dynamic air atmospheres, as indicated by the characteristic shift of the oxalate band at 815 cm^{-1} on dehydration. A transformation of CrC_2O_4 to CrO was also detected. A separate phase of CrO could not be obtained; this compound always occurred with CrC_2O_4. Thus the transformation of CrC_2O_4 to CrO seems to be an equilibrium reaction. This mixture of CrO and CrC_2O_4 is then transformed to Cr_3O_4 (i.e. $CrO_{1.33}$). The final step is the decomposition of Cr_3O_4 to Cr_2O_3, in all three atmospheres. In this step, the intimately associated oxygen is probably responsible for the formation of Cr_2O_3.

It has been reported in the literature [13] that as the $M–O_I$ bond (Scheme 1) becomes stronger, so the $C–O_I$ bond is lengthened and the $C–O_{II}$ bond is shortened. The final product in the present work, Cr_2O_3, was produced in a nitrogen atmosphere. The decomposition temperature represents the energy required to break the $C–O_I$ bond, and this will depend less critically on the nature of the cation.

CONCLUSIONS

The results of the present study allow us to make the following important observations regarding the solid state decomposition of $CrC_2O_4 \cdot 2H_2O$.

(a) Dehydration of $CrC_2O_4 \cdot 2H_2O$ yielding anhydrous CrC_2O_4 took place in all three of the atmospheres considered.

(b) Conventional thermal analysis curves (TG, DTA and DTG) showed a very broad and large exothermic peak (DTA) and a continuous weight loss (TG) for the oxalate in all three atmospheres at the oxidative decomposition step. These curves could not, however, provide information regarding the types of intermediates formed at this step. Hence it was found necessary to supplement these results with a more helpful technique, i.e. use of d.c. electrical conductivity measurements, in conjunction with IR spectral and X-ray diffraction investigations.

(c) In dry nitrogen, the plot of log σ vs. T^{-1} showed a well characterized step corresponding to dehydration. The formation of CrO and Cr_3O_4 as intermediates was confirmed; CrO is always formed together with CrC_2O_4.

(d) The final product of decomposition, in all three atmospheres, was found to be Cr_2O_3.

(e) Gas chromatograms showed that polar gases were present during the thermal decomposition of $CrC_2O_4 \cdot 2H_2O$.

ACKNOWLEDGEMENTS

This work was undertaken with financial support from Grants-in-Aid (Ministry of Defence), Government of India. A junior fellowship has been awarded to M.M.R. The teacher fellowship scheme, U.G.C., New Delhi, has been awarded to A.D.A. The authors wish to thank the late Professor A.J. Mukhedkar, and Dr. Mrs. V.A. Mukhedkar and Dr. S.B. Kulkarni of the Department of Chemistry for their suggestions and stimulating discussions.

REFERENCES

1 A.R. Burwell, Jr., G.L. Haller, K.C. Taylor and J.F. Read, Adv. Catal., 20 (1969) 1.
2 A. Zecchina, S. Coluccia, E. Guglielminotti and G. Goitti, J. Phys. Chem., 75 (1971) 2774.
3 K.S. Rane, A.K. Nikumbh and A.J. Mukhedkar, J. Mater. Sci., 16 (1981) 2387.
4 A. Venkataraman, V.A. Mukhedkar, M.M. Rahman, A.K. Nikumbh and A.J. Mukhedkar, Thermochim. Acta, 112 (1987) 231.
5 A. Venkataraman, V.A. Mukhedkar, M.M. Rahman, A.K. Nikumbh and A.J. Mukhedkar, Thermochim. Acta, 115 (1987) 215.
6 M.M. Rahman, V.A. Mukhedkar, A. Venkataraman, A.K. Nikumbh, S.B. Kulkarni and A.J. Mukhedkar, Thermochim. Acta, 125 (1988) 173.
7 R.B. Fahim, M.I. Zaki and N.H. Yacoub, J. Colloid Interface Sci., 88 (1982) 502.
8 A.C. Zettlemoyer, M. Siddique and F.J. Micale, J. Colloid Interface Sci., 66 (1978) 173.
9 K. Muraishi, K. Nagase and N. Tanaka, Thermochim. Acta, 23 (1978) 125.
10 D. Dollimore, J.P. Gupta and D.V. Nowell, Thermochim. Acta, 30 (1979) 339.
11 C.R.M. Rao and P.N. Mehrotra, J. Chem. Tek. Biot., 29 (1979) 578.
12 J.E. House, Jr., and T.G. Blumthal, Thermochim. Acta, 36 (1980) 79.

13 D. Dollimore, D.L. Griffiths and D. Nicholson, J. Chem. Soc., (1963) 2617.
14 E.D. Macklen, J. Inorg. Nucl. Chem., 30 (1968) 2689.
15 U.B. Ceipidor, G. D'Ascenzo, M. Tomassetti and E. Cardarelli, Thermochim. Acta, 30 (1979) 15.
16 H. Lux and G. Illmann, Chem. Ber., 91 (1958) 2143.
17 H. Lux and G. Illman, Chem. Ber., 92 (1959) 2364.
18 J. Fujita, A.E. Martell and K. Nakamoto, J. Chem. Phys., 36 (1962) 324.
19 J. Fujita, A.E. Martell and K. Nakamoto, J. Chem. Phys., 36 (1962) 331.
20 M.A. Khilla, Z.M. Hanafi and A.K. Mohamed, Thermochim. Acta, 54 (1982) 319.
21 ASTM File, No. 6-532.
22 M.A. Khilla, Z.M. Hanafi and A.K. Mohamed, Thermochim. Acta, 56 (1982) 291.
23 ASTM File, No. 6-504.
24 ASTM File, No. 12-559.